Dalton Transactions

Accepted Manuscript

ROYAL SOCIETY OF CHEMISTRY

www.rsc.org/dalton

Surface Modification of Layered Zirconium Phosphates: A Novel Pathway to Multifunctional Materials

*Brian M. Mosby, Agustín Díaz, and Abraham Clearfield**

[*] B.Mosby, Dr. A. Díaz, Dr. A. Clearfield
Department of Chemistry
Texas A&M University
PO Box 30012, College Station, TX 77842-3012, USA

KEYWORDS: Self-assembled monolayers, Inorganic Layered Materials, Nanomaterials, Nanocomposites, Drug delivery, Pickering emulsions.

Abstract. The intercalation of inorganic layered materials has resulted in a wide range of applicability. In such cases the applicability of the material is largely dependent upon the species intercalated within the layer, and the layered material acts largely as a host. Recently, the surface modification of inorganic layered materials has been investigated and it has been shown that the exterior layers can be exclusively functionalized. The advent of surface chemistry allows for the synthesis of particles with both a controlled interlayer and surface. This approach can be used to tailor nanoparticles for specific applications. Herein we review the surface chemistry of α-zirconium bis(monohydrogen orthophosphate) monohydrate ($Zr(HPO_4)_2 \cdot H_2O$, α-ZrP) along with some applications of

recent interest. Not only can these reactions be applied to α-ZrP, but similar chemistry can also be expanded to other layered materials and systems.

1. Introduction

Early History

Zirconium phosphate is obtained as a gelatinous amorphous precipitate by adding an excess of phosphoric acid to a soluble zirconium salt.[1] It was discovered that the solid was a cation exchanger through the continual discovery of some of the impurities present in the solution within the precipitate.[2] This property led to extensive investigation, in the early days of atomic energy development, as to the ability of the solid to remove radioisotopes from reactor cooling waters.[3, 4] Early structural representations of the gels represented them as zirconyl compounds[5] such as $ZrO(H_2PO_4)_2$. In 1964 crystalline forms of zirconium phosphate were prepared by refluxing the gel in phosphoric acid solutions.[6] Its formula was determined to be $Zr(HPO_4)_2 \cdot H_2O$; shortly thereafter the crystal structure was determined and refined to reveal a layered compound.[7,8]

Subsequently a second layered form of zirconium phosphate was discovered.[9] The structure was partially determined for the titanium phase[10] and later fully determined for the Zr compound.[11] It was therefore necessary to distinguish these two forms; the compound $Zr(HPO_4)_2 \cdot H_2O$ was designated as α-ZrP and the second compound of formula $Zr(PO_4)(H_2PO_4)_2 \cdot 2H_2O$ was designated as γ-ZrP.

The Structure and Nano Nature of Zirconium Phosphates

The structures of α and γ ZrP are now well known and have been often described.[11-14] Here we provide some of the essentials necessary to the present narrative. In the α-phase structure, the Zr ions are slightly above and below the midpoint of the layer. They are six coordinate, bonding to six oxygen atoms from six different phosphate groups. The bonding requires that each phosphate group coordinates to three different Zr ions; the remaining oxygen atom of the phosphorus is protonated. The hydroxy phosphate groups terminate the surface or exist as double rows of P-OH groups in staggered arrays between the layers (**Figure 1**). The bonding scheme produces a layered compound with a 7.6 Å interlayer distance.

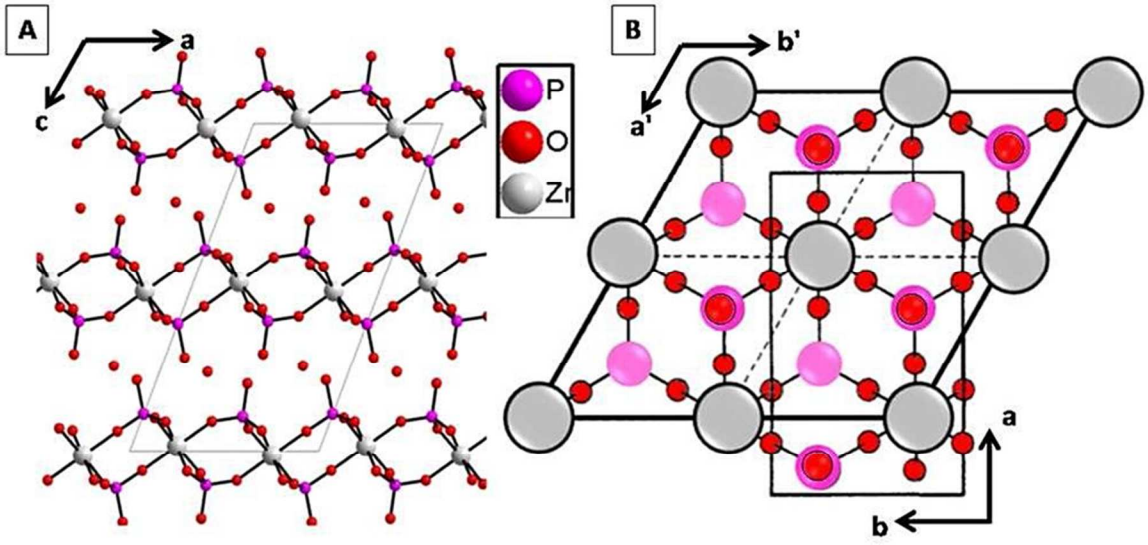

Figure 1: (A)A representation of the α-ZrP structure displaying the connectivity of the layered compound and (B) the surface of the layers. The hydrogen atoms are omitted for clarity. Taken from: Agustín Díaz; Brian M. Mosby; Vladimir I. Bakhmutov; Angel A. Martí; James D. Batteas; Abraham Clearfield; *Chem. Mater.* **2013,** 25, 723-728. DOI: 10.1021/cm303610v

γ-ZrP has a very different structure from that of α-ZrP. In the case of γ-ZrP the Zr ions are six coordinate, but there are two types of ligands: a phosphate group, PO_4^{3-}, and a dihydrogen phosphate group, $H_2PO_4^-$. The phosphate group and the Zr^{4+} ions lie within the layers with the four oxygen atoms bonding to four Zr ions. These ZrO_4 groups are then bridged top and bottom to each other while the remaining $P(OH)_2$ groups are located in the interlayer region and on the surface. The interlayer distance is 12.4 Å and the two interlayer water molecules form a hydrogen-bonding network, creating stabilizing interactions among the layers.

A defining feature of both α and γ ZrP is their propensity to form as nanoparticles. In the case of α-ZrP, crystals were prepared by reflux of the amorphous gel in phosphoric acid of increasing concentration for 48 hours.[15] The first signs of structure occurred for 0.5 M H_3PO_4. In this case, the interlayer distance was ~11 Å due to five moles of water between the layers. The measured thickness was 70 Å, which amounts to approximately six layers and the length of the particles was about 100 nm as determined subsequently.[16] By increasing the concentration of H_3PO_4, the temperature, or addition of HF, it is possible to control the size of the α-ZrP particles from 50 nm to large single crystals[16, 17]

Recently, a new method of preparation of α-ZrP has been reported.[18] Zirconyl propionate, $ZrO_{1.26}(C_2H_5COO)_{1.49}$, was dissolved in alcohol (ethanol, propanol or butanol) and concentrated H_3PO_4 was added to produce the desired H_3PO_4:Zr ratio (2:1, 4:1, or 6:1). Gels formed within minutes, which were washed with the same alcohol used in the preparation and dried at 60°C to produce a white powder. The X-ray powder diffraction patterns of the gels indicated the formation of a layered α-ZrP structure with

the alcohol encapsulated within the layers. The broadened peaks indicate a small particle size, which was determined to be 40 nm by electron microscopy.

γ-zirconium phosphate is also obtained as nano-sized particles. In fact, the structure determination of the compound was initially unsuccessful due to the poor quality of the X-ray powder patterns. To improve the quality, the mixture of $NaH_2PO_4 \cdot H_2O$, H_3PO_4 and $ZrOCl_2 \cdot 8H_2O$ was refluxed for 72 h and subsequently transferred into a pressure vessel and reacted at 190°C for 120 h. The structure of the resulting material was then solved using the powder diffraction pattern.[11]

It was found that organic derivatives of α-ZrP could be achieved by substituting phosphoric acid with phosphonic acids or phosphoric acid esters.[19] In such cases the inorganic structure is retained, however the hydroxyl groups are replaced with alkyl or aromatic groups. Zirconium phenyl phosphonate was first prepared by Alberti et al.[19] However, the X-ray powder pattern contained only a few broad peaks indicative of the small particle size. Particles prepared hydrothermally at 140°C for three days were shown to range from 20-60 nm and to be as thin as 7 nm.[20] The structure was solved through a collaborative effort between Prof. Alberti and Prof. Clearfield. Alberti prepared a highly crystalline sample of $Zr(O_3PC_6H_5)_2$ that was heated for 30 days at 200°C. The sample was then sent to the Clearfield research group and the structure was solved using powder diffraction data obtained from synchrotron radiation.[21] The structure is very similar to that of α-ZrP except that the phenyl rings are tilted 30° relative to the perpendicular between the layers (**Figure 2**). It is also possible to prepare mixed derivatives such as zirconium phenyl, methyl phosphonate.[20] In such cases the greater the amount of second ligand added the smaller the particle size.[22]

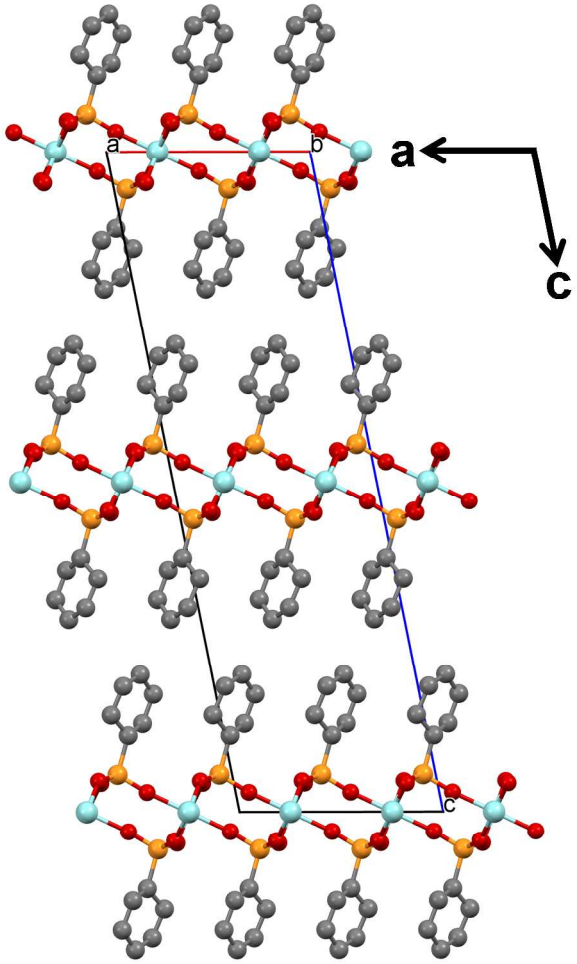

Figure 2: Representation of $Zr(O_3PC_6H_5)_2$ along the b axis showing its unit cell and the layered structure.

Finally, we may mention the UMOFs that are layered zirconium or Sn(IV) compounds in which the layers are crosslinked by bisphosphonic acids.[23] They are porous and may be functionalized by inclusion of a second ligand. The monoligand particles are in the 90-100 nm range but as more of a second ligand is incorporated the particle size decreases to as small as 20-25 nm in size.

Surface Functionalization of α-ZrP

During the last 50 years extensive research has evolved around the chemistry of both α and γ ZrP with thousands of published papers. The tunability of their size, aspect ratio, ion exchange properties and intercalation ability has led to numerous applications in fuel cells,[24] electron transfer reactions,[25, 26] surface adsorption of proteins,[27] lubricant additives,[28] and catalysis among others.[29] Surface functionalization of the particles has recently emerged as a new area of focus. Originally it was demonstrated that isocyanates could be bonded to the exterior of α-ZrP nanoplatelets.[30] Exfoliation of the functionalized material led to a mixture of Janus and Gemini particles that were used as stabilizers in Pickering emulsions. Both ethoxy and chlorosilanes react with the surface of ZrP as well. The attachment of octadecyltrichlorosilane (OTS) to the surface of α-ZrP led to hydrophobic particles, which were dispersible in non-polar solvents.[14] α-ZrP intercalated with a photoactive molecule was surface modified with OTS and used to conduct photo-induced electron transfer in non-polar media. It has also been demonstrated that epoxides can be covalently attached to the surface of α-ZrP.[31] In this case the synthesized particles were used as fillers in a polymer matrix. Additionally, it was shown that intercalation of the modified particles could be used to add functionality to the composites. More recently, it was demonstrated that the ion exchange chemistry of α-ZrP could be used to deposit metal ions exclusively on the surface of the nanoparticles. The metal ion layer can then be functionalized with phosphonic acids, resulting in surface functionalized ZrP.[32]

ZrP has been demonstrated to be a versatile material in which multiple reactive groups can be used to modify the same surface (**Figure 3**). Although surface modification has been demonstrated as a viable method of imparting organic functionality to α-ZrP, there are several key issues that still need to be addressed. Prevalent issues include the affects of the reactive group or the particle size on the surface modification and a thorough characterization of α-ZrP that is both intercalated and surface modified. This perspective will seek to investigate these areas.

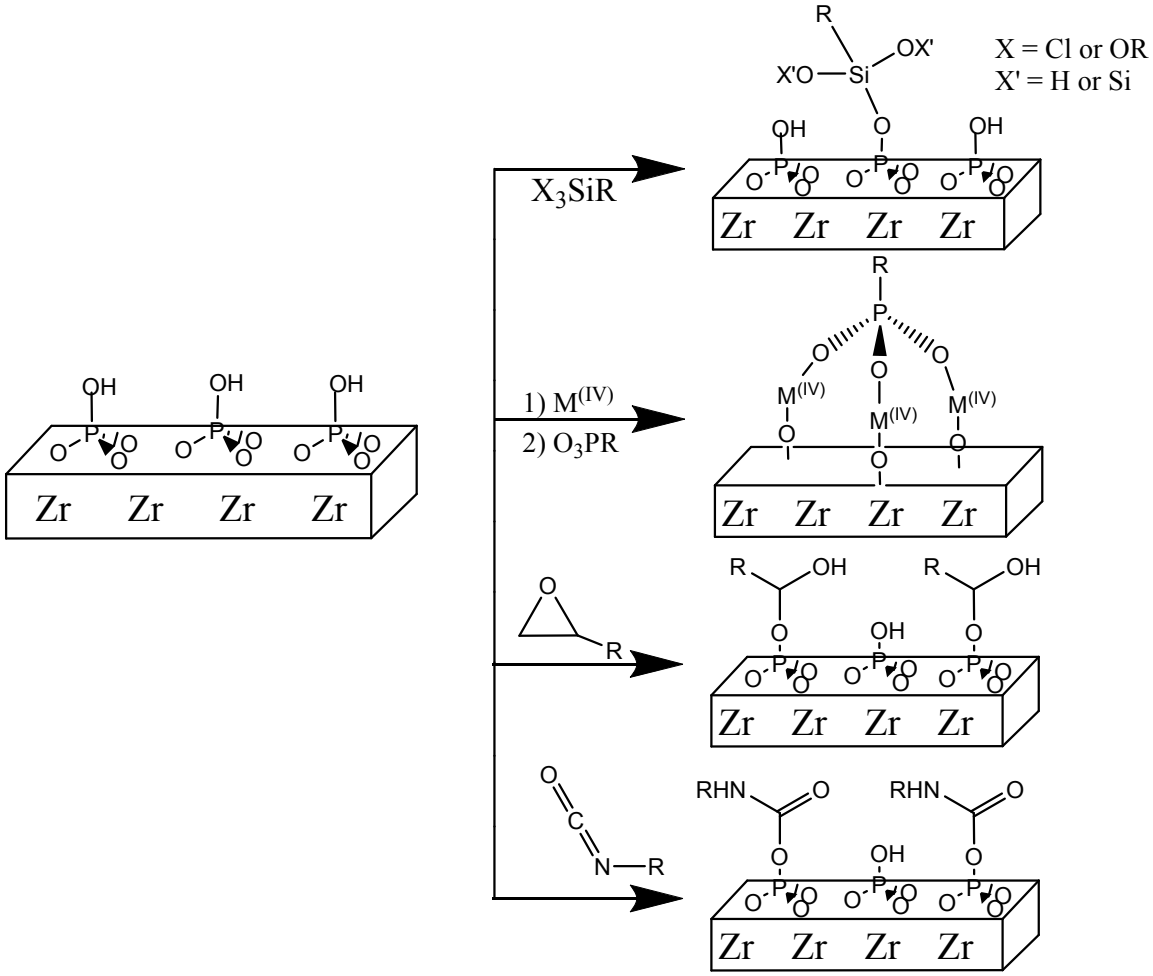

Figure 3: Reaction scheme of select α-ZrP surface modification reactions. In this case the scheme shows the reactions of silanes, tetravalent metal ions followed by the coordination of phosphonic, epoxides, and isocyanates.

2. Overview of α-Zirconium Phosphate Surface Chemistry

Each of the prevalent α-ZrP surface reactions will now be reviewed using the 18 carbon derivative of silanes (octadecytrichlorosilane, OTS), phosphonic acids (octadecylphosphonic acid, ODPA), epoxides (1,2-epoxyoctadecane, EOD), and isocyanates (octadecylisocyanate, ODI). The X-ray powder diffraction (XRPD) of the modified samples all display largely identical diffraction patterns indicating that none of the modifiers had any interaction with the interlayer region of the α-ZrP.[14,

[31, 32] Since only the exterior layers are modified, observation of structural changes are not expected in XRPD. In contrast, the FTIR spectra of the modified samples display differences depending on the reactive group used for functionalization (**Figure 4**). This is primarily observed in the case of the isocyanate and the epoxide modified samples. The epoxide is known to bond by nucleophilic attack of the phosphate group to the epoxide ring.[33] The reaction results in formation of P-O-C bonds and thus phosphate esters; the ester can be observed in the FTIR spectrum of the epoxide modified sample at *ca* 940 cm^{-1}.[31] Similarly, the FTIR spectrum of the isocyanate modified sample indicates bonding to the α-ZrP base. The disappearance of the isocyanate stretch at 2260 cm^{-1} and the appearance of the characteristic stretching and bending bands of the carbamic phosphoric group formed by the reaction of the isocyanate with the surface phosphates at 3310 cm^{-1} (N-H stretch) and 1650-1350 cm^{-1} (C=O stretching and N-H bending modes) respectively, are indicative of the reaction of the isocyanate group to the α-ZrP surface.[34] It is important to mention that in all the cases the stretching bands for the interlayer water are still present, indicating that the modifier has not interacted with the interlayer region. However, in some cases the stretching band corresponding to the interlayer water is diminished or deformed due to partial dehydration of the water molecule from the interlayer.[31] The dehydration is a result of the extended reflux at high temperatures used for the surface modification reaction. The distinct signals due to covalent attachment of the modifiers, the alkyl stretching observed, and the interlayer water molecule suggest the exclusive modification of the surface of α-ZrP.

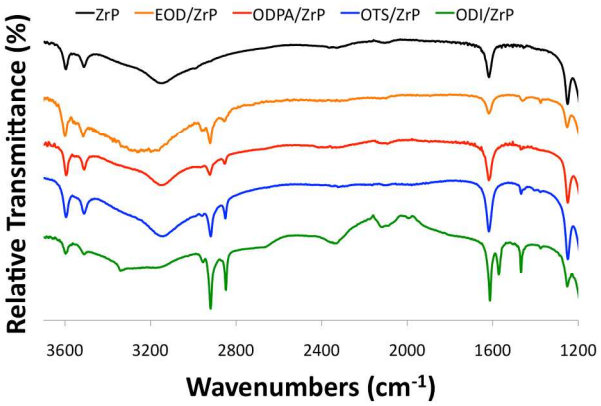

Figure 4: FTIR of pristine α-ZrP and α-ZrP modified with octadecytrichlorosilane (OTS), octadecylphosphonic acid (ODPA), 1,2-epoxyoctadecane (EOD), and octadecylisocyanate (ODI).

TGA can be used to determine the uptake of the various ligands on the surface. As all other variables are constant, the material with the largest weight loss will have the highest uptake of modifier on the surface. Examination of the TGA thermograms reveal that in all cases the surface has been successfully modified (**Figure 5**). The uptake of the isocyanate was found to be the highest, which is reasonable, as isocyanates are known to be extremely reactive. Also, a substantial amount of isocyanate is able to bond to the surface because the formation of the carbamic phosphoric groups minimizes steric hindrance. The weight loss exhibited by the epoxide modified sample is the second highest, the epoxides interact with the surface phosphate groups in a one to one fashion so a relatively high uptake is expected. The weight losses of the OTS and ODPA modified ZrP are both very similar. It should be noted that in both cases the organic molecule is attached to another atom and does not interact directly with the surface. The addition of Si or a M(IV) ion incorporates mass that does not thermally decompose and thus adds

additional weight to the thermo decomposed product; as a result the total percent weight losses are also much lower. Investigation of the first derivative of the weight loss of the thermograms reveals that the loss of the organic modifier can exist as either one or two events and that the temperature at which the loss occurs can fluctuate. The isocyanate weight loss occurs in two events, the first weight loss is the highest and is expected to be the isocyanate bound to the surface whereas the second weight loss corresponds to the isocyanate attached to the edges that is slightly more stable as the interlayer provides some protection from thermal degradation. Also, in the case of the epoxide two weight loss events are observed in which the second is clearly dominant. It has been reported that epoxides have two bonding conformations with α-ZrP, the predominant product, in which the ring opening results in the formation of a secondary alcohol and the minor product, in which a primary alcohol is produced .[33] It is likely that these two weight losses correspond to the two bonding conformations. The weight loss occurs as a single event in the remaining two samples and it appears that the ODPA is slightly more stable than the OTS.

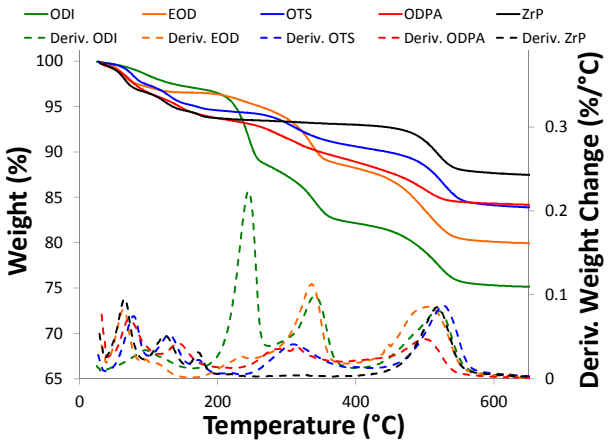

Figure 5: TGA of pristine α-ZrP and α-ZrP modified with octadecytrichlorosilane (OTS), octadecylphosphonic acid (ODPA), 1,2-epoxyoctadecane (EOD), and octadecylisocyanate (ODI).

Lastly, NMR can be used to probe the environments of phosphorus within the compounds to determine if bonding has in fact occurred. The ^{31}P NMR spectra of all the modified samples contain similar features of α-ZrP but the phosphorus environments for bond formation differ somewhat, **Figure 6**. The common signals within all the samples are at *ca.* -17 ppm, -19 ppm, and -21 ppm and can be attributed to the α-ZrP starting material as discussed thoroughly elsewhere.[32] In the case of epoxides phosphate ester formation is observed at *ca.* -22 ppm. Magnification of the silane modified material shows a small signal at *ca.* -31 ppm corresponding to P-O-Si bond formation. The isocyanate modified sample displays a dominant signal that occurs at *ca*. -21 ppm suggesting that the nanoparticles have been mostly dehydrated. A signal also occurs at *ca.* -22.6 corresponding to phosphate ester formation as in the epoxide case. Additionally, there may be a small

shoulder present at *ca.* -24 ppm as a result of the interaction of the amine of the carbamic acid formed with the phosphate on the surface via hydrogen bonding. The intensity of the signals indicates that there is much more bond formation in the isocyanate and epoxide case than in the silane. Surface modification with silanes results in only a few P-O-Si bonds, evidenced by the weak signal at *ca.* -31 ppm. It is proposed that siloxane bond formation from the surface bound silica accounts for most of the coverage. In regards to the ODPA modified ZrP, the ODPA does not interact directly with the ZrP surface therefore covalent attachment is not observed as in the other cases. The ODPA is coordinated to metal ions that are interacting with the surface through ion exchange, as a result no alternation in the base ZrP signals are observed. [32]

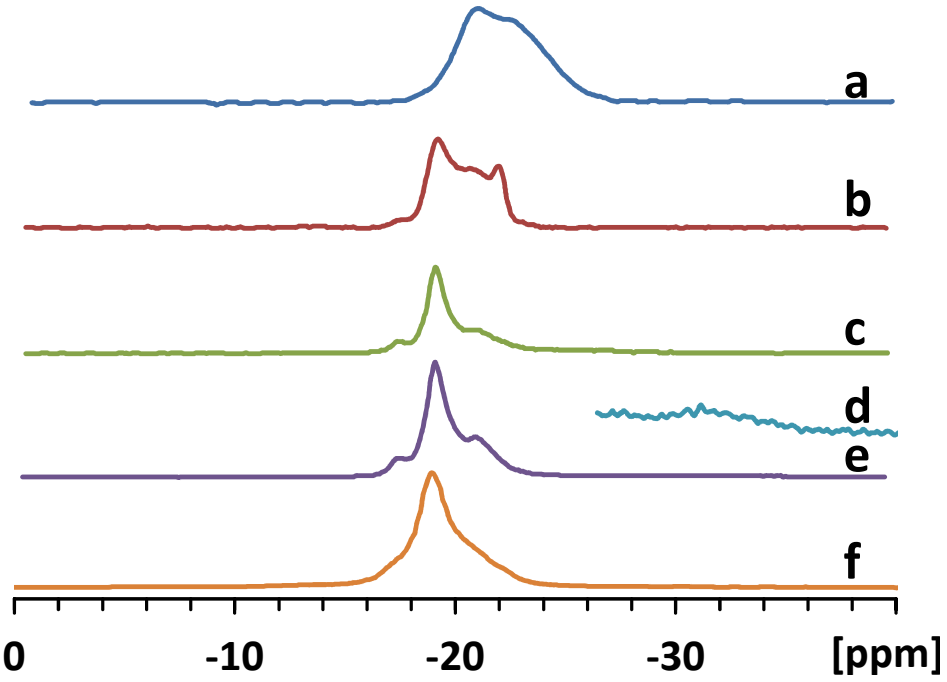

Figure 6: ^{31}P NMR of α-ZrP surface modified with (a) octadecylisocyanate (ODI) , (b) 1,2-epoxyoctadecane (EOD), (c) octadecylphosphonic acid (ODPA), (d) octadecyltrichlorosilane (OTS) 4x magnification, and (e) octadecyltrichlorosilane (OTS) full spectrum along with (f) pristine α-ZrP.

3. Particle Size Effects

It has been confirmed that multiple reactive groups can be used to modify the surface of α-ZrP. It is now of interest how the size of the particles affects the surface modification reaction. The synthesis of α-ZrP using various concentrations of phosphoric acid has previously been reported and it is known that increasing the acid concentration produces more crystalline materials.[35] The surface modification reaction of ZrP and the epoxide ,1,2-epoxyoctadecane, was investigated using α-ZrP of low (3M), medium (6M), and high (12M) crystallinity prepared by the reflux method.

The infrared spectra of the modified samples agree well with those discussed previously. It is expected that as the α-ZrP becomes more crystalline both the particle size and thickness will increase, which will decrease the percentage of phosphorus available for modification leading to a smaller contribution of organic in the sample and a corresponding decrease in the signals associated with the modification. The initial area of interest is that of the alkyl stretching of the 1,2-epoxyoctadecane. The stretching bands due to the alkyl chain can be observed in the low, medium, and high crystallinity cases suggesting that modification successfully occurred in all samples. It can be noted however that the intensity of the stretching is substantially lower in the medium and high crystallinity cases as compared to the low crystallinity sample. This is reasonable as the low crystallinity particles are expected to be *ca.* 11 layers thick whereas the highly crystalline material is estimated to be *ca.* 50 layers thick. The medium and highly crystalline samples appear to display similar stretching due to modification in both the alkyl region and phosphate ester region. Further investigation of the phosphate ester region shows that in all cases the signal corresponding to ester formation can be observed. This suggests that in the reflux case that there are still a significant amount of phosphates on the surface relative to those in the interlayer.

The TGA thermograms of the three modified samples follow the expected trend, as the highest weight loss is observed for particles with low crystallinity and the lowest weight loss for the highly crystalline samples, **Figure 7.** As with all modified samples there are four main weight loss regions corresponding to the surface solvent and water, interlayer water, the organic modifier, and the

condensation of the phosphate to pyrophosphate. Initially, it can be seen that the amount of surface water differs in all the samples. The particles with low and medium crystallinity both display water absorbed to the surface whereas the more crystalline particles do not exhibit this weight loss. Secondly, weight loss corresponding to the interlayer water molecule differs as well. There are two peaks in the second derivative, which correspond to the interlayer water molecule. The first can be said to be the solvent and water that is held loosely by the particles, mostly on the edges whereas the second is the intercalated water that is deeper within the core of the particles held by hydrogen bonds with the phosphate groups of the interlayer. The trend shows that the more crystalline the particles become, the less significant is the first peak and the more dominant the second becomes. More crystalline particles have a stronger attraction between the layers and thus hold the water molecule more efficiently; in addition more crystalline particles have a higher number of layers, which leads to more internal surface area and intercalated water. The derivative of the water loss also shows that the dehydration behavior of the low and medium crystalline samples is very similar. The derivative corresponding to the modifier exists in two steps, however it appears that the first and not the second peak is the dominant process in all cases except the 3M. The inversion of intensity of the two derivative processes suggests the bonding of the epoxide to the surface differs somewhat amongst different particle sizes. Lastly, it can be noted that the peak corresponding to the condensation is shifted in all cases; however this is a function of the crystallinity of the particles and not the modification.

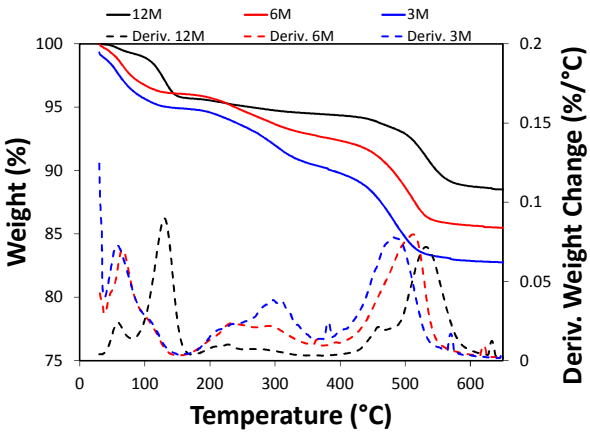

Figure 7: (A) TGA and derivative of weight loss of EOD/ZrP synthesized with reflux α-ZrP of low (3M), medium(6M), and high crystallinity(12M).

TGA has successfully confirmed that the organic contribution of all the samples is different and therefore modification has occurred to different extents in all the samples. Solid state ^{31}P NMR was utilized to probe the overall effect of the modification on the environment of the phosphorus atoms in the base ZrP structure. Based on previous experiments it is expected that in the case of successful modification by reflux that four signals will be observed in the ^{31}P NMR, the two original signals observed corresponding to α-ZrP and two additional signals at -21.4 and -22.4 ppm corresponding to the dehydration of α-ZrP and the formation of a phosphate ester.[31] All four of these signals are observed in the modified materials regardless of crystallinity, **Figure 8**. It can clearly be observed that as the particles become more crystalline the signal corresponding to the orthophosphate (-19 ppm) becomes more dominant and all other signals decrease in intensity. Integration of the signals shows that the percentage of phosphorus that is modified decreases as the particles become thicker. The signals corresponding to ester formation and thus

surface modification (- 22 ppm) account for 19.1%, 13.3%, and 9.6% for the low, medium, and high crystallinity samples respectively. All remaining phosphorus environments are attributed to the base α-ZrP material. This corroborates with the TGA data that suggest the uptake of epoxide on the surface is less significant as the particles increase in size. The aliphatic chains of the epoxide can also be observed by ^{13}C NMR, confirming the successful modification.[31] It was observed that signals corresponding to the covalent attachment of the epoxide to ZrP decreased in intensity as the particles became more crystalline.

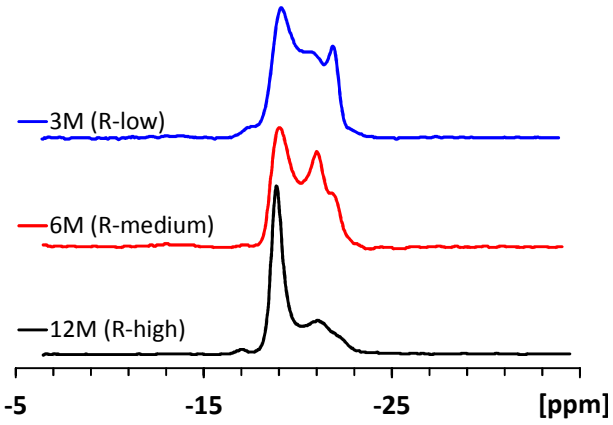

Figure 8: ^{31}P NMR of EOD/ZrP synthesized with reflux α-ZrP of low (top), medium (middle), and high (bottom) crystallinity.

Similar experiments were also carried out with micron-sized α-ZrP prepared by the hydrothermal method. In this case it was found that evidence of modification was only found in the FTIR of the lowly crystalline cases. TGA and NMR were not effective at monitoring the modification due to the large amounts of interlayer phosphates present. This suggests that although surface modification is possible in

all cases, there is a maximal thickness, after which the modification will not be observable by traditional characterization methods.

4. Multifunctional ZrP: Combining Intercalation and Surface Modification

Inorganic-organic hybrids have been synthesized from α-ZrP before;[12, 33, 36-38] however the current approach differs as the phosphate functionality of the interlayer is retained. The retention of the exchangeable phosphates in the interlayer allows for further modification of the particles through intercalation. Although a few examples of multifunctional α-ZrP have been reported previously, the focus was on the applicability of the materials.[14, 31] As a result a thorough characterization of the multifunctional particles has been lacking. We now present the characterization of multifunctional ZrP based materials, confirming that they are both surface modified and intercalated.

Initially, Rhodamine 6G (Rho-6G) was intercalated within the layers of α-ZrP. XPRD of the intercalated sample revealed an interlayer spacing of 19.4 Å, verifying the successful intercalation of Rho-6G into the interlayer of the α-ZrP. The powder pattern of the epoxide surface modified product displays the same reflections as the starting material indicating that leaching of the Rho-6G from the interlayer or unwanted interactions of the epoxide with the interlayer region did not occur, **Figure 9**.

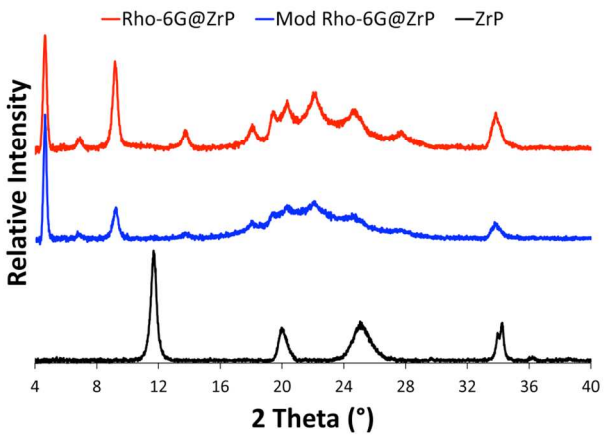

Figure 9: XRPD of α-ZrP and Rho-6G@ZrP before and after modification with EOD.

The FTIR spectrum of Rho-6G@ZrP is comprised of stretches representative of α-ZrP and Rho-6G, where Rho-6G dominates the spectrum due to the apparent high loading of the molecule within the interlayer. In addition Rho-6G has alkyl, aryl, amino, and imine groups therefore the majority of the bands in the spectra can be attributed to Rho-6G. Upon completion of the surface modification reaction the spectrum does not change significantly, **Figure 10**. Close examination of the spectrum of the modified sample shows that the alkyl stretching bands are considerably stronger in the modified sample than in the pure intercalation compound. Although the intensities in FTIR spectra are not necessarily comparable in all cases, this can be taken as evidence that the modifier did in fact interact with the surface of the Rho-6G@ZrP nanoparticles.

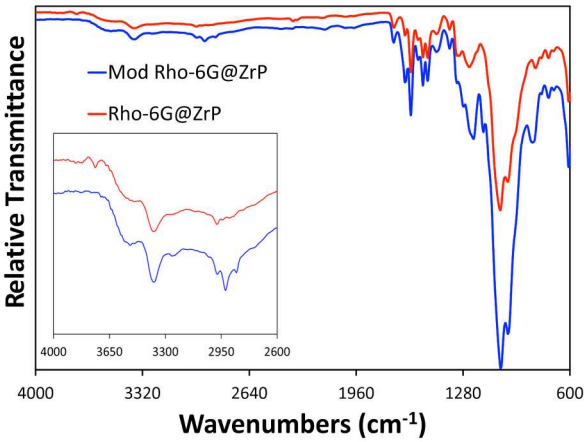

Figure 10: FTIR of Rho-6G@ZrP before and after modification with EOD. The inset shows a magnified view of the alkyl stretching.

To verify the attachment of the epoxide to the surface of the nanoparticles TGA was performed. The TGA thermogram of Rho-6G@ZrP displays a total weight loss of 50.26% and calculations reveal that this is representative of 0.45 moles of Rho-6G relative to Zr in the compound. As is typical, surface water, solvent, and interlayer water is lost below 100°C. The decomposition of the Rho-6G occurs in three distinct steps (**Figure 11**). The first from 305°C to 335°C, the second from 445°C to 515°C, and the last from 565°C to 620°C. The first step is the least intense of them whereas the second is the most dominant. It is likely that the second step is the decomposition of the bulk of the Rho-6G, while the last step is the condensation of the phosphates mixed with the residual Rho-6G that is yet to decompose. The TGA thermogram of the modified Rho-6G@ZrP follows the same pattern with the exception of a new weight loss event occurring from 175°C to 205°C, corresponding to the epoxide modifier, **Figure 11**. It is therefore confirmed by TGA that the surface of the particles was successfully modified.

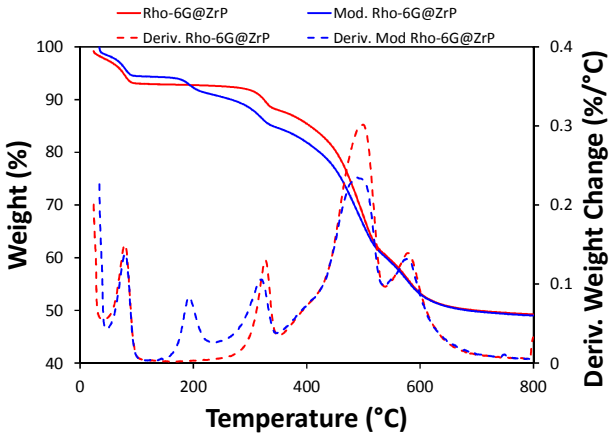

Figure 11: TGA of Rho-6G@ZrP before and after modification with EOD.

Previous experiments have shown that the surface modification of pristine α-ZrP with 1,2-epoxyoctadecane results in the attachment of 0.14 moles of epoxide to the surface. The extent of surface modification and the thermal stability of the epoxide modifier in pristine α-ZrP will now be compared to that of the intercalated samples. **Table 1** displays the calculated formulas for a series of modified samples. It can be observed that there is some slight variation in the amount of modifier in the intercalated α-ZrP, however in all cases the surface is successfully modified. The data shows that intercalated samples with lower loadings tend to uptake more surface modifier than those with higher loadings. Additionally, there is not a significant difference between the uptake in the low loading samples and the pristine α-ZrP. It can also be noted that as is the case with the pristine α-ZrP, the derivative of the weight loss corresponding to the epoxide occurs in two steps suggesting that the bonding is identical in both cases.

Observation of the thermal decomposition of the epoxide on the surface in the samples shows slight fluctuations of the temperature range depending on the interlayer molecule, **Table 1**. This data could possibly suggest that the increase in the loading level within the particle causes somewhat of a destabilization of the surface. The exterior or surface layers of α-ZrP possess a set of phosphate groups on the surface and another set in the interlayer; electronically these phosphates are connected. It is plausible, if the interlayer phosphate groups are engaged in a considerable amount of ionic interaction due to intercalation, that the surface phosphates of that layer may have less electron density and therefore form weaker, less stable bonds. In comparison to the compounds intercalated via the ion-exchange mechanism, it can be noted that the decomposition temperature of the epoxide in modified Rho-6G@ZrP is substantially lower. In fact, in this case the decomposition of the epoxide is completed before the decomposition even begins in the other cases. However, it cannot be said with certainty whether this occurrence is the result of the high loading of the Rho-6G@ZrP, the acid-base intercalation mechanism, or a combination of both. In comparison to the pristine modified α-ZrP the weight loss ranges exhibited in the intercalated materials are similar for $Ru(bpy)_3^{2+}$@ZrP, however as the loading of the intercalated molecule increases the stability shifts to lower temperatures. This topic is essential to understanding the stability of multifunctional α-ZrP and is currently under investigation.

Table 1: Calculated formulas for the multifunctional α-ZrP along with other thermal data. The modifier is EOD in all cases.

Modified	Formula	Weight Loss Range (°C)	T at Derivative Peak Maxima (°C)
ZrP	$Zr(H_{0.861}PO_4)_2(Mod)_{0.139}\cdot 0.6\ H_2O$	166-380	288/336
$Ru(bpy)_3^{2+}$@ZrP	$Zr(H_{0.91}PO_4)_2\,(Ru(bpy)_3)_{0.09}(Mod)_{0.13}\bullet\ 1.4\ H_2O$	188-326	262
$Fe(phen)_3^{2+}$@ZrP	$Zr(H_{0.84}PO_4)_2\,(Fe(phen)_3)_{0.16}(Mod)_{0.06}\bullet\ 1.4\ H_2O$	183-306	270
Rho-6G@ZrP	$Zr(H_{0.66}PO_4)_2\,(Rho\text{-}6G)_{0.44}(Mod)_{0.08}\bullet\ 1.4\ H_2O$	144- 230	193

5. Some Applications of α-ZrP

As mentioned earlier the ability to intercalate reactive species between the layers of ZrP provides for applications, such as catalysis, photoinduced charge separation, drug delivery, polymer nanocomposite, biosensors, and fuel cells, among many others. In order to improve the applicability of these materials surface modification of the nanoplatelets is highly desirable. Below are presented some examples of applications and possible applications of surface modified α-ZrP nanoparticles.

Electron Transfer Reactions

In order to understand in depth how the surface coverage and the accessibility of different species affects the internal layered nanoparticles, after surface modification, an electron transfer reaction was performed. The kinetics of the electron transfer reaction were studied following the Stern-Volmer model, where $Ru(bpy)_3^{2+}$@ZrP, the photoinduced electron donor, was surface modified by covalent attachment of three different surface modifiers (OTS, ODI and EOD) and p-benzoquinone (p-BQ) served as the electron acceptor. The $Ru(bpy)_3^{2+}$@ZrP nanoparticles were functionalized with their respective surface modifiers under

identical conditions. A 0.01% (w/v) suspension of the nanoparticles was prepared in 1,2-dichlorobenzene, to which a known volume of p-BQ solution was added. **Figure 12** shows the Stern-Volmer plot of the three different systems quenched by p-BQ. The Stern-Volmer plot shows a quenching mechanism typical of a mixed quenching process, where dynamic and static quenching are both present in the electron transfer reaction for all the surface modified derivatives. We expect that the extent of the surface coverage, concentration of electron donor in the layer, the solvent used, and the initial concentration of the quencher will affect the mechanisms, making one more favorable at a certain point. The system itself is quite complex, where possible co-intercalation of the quencher into the layers, along with the $Ru(bpy)_3^{2+}$ could take place. This phenomenon is responsible for part of the static quenching observed in all three cases. Nevertheless, the cointercalation of the p-BQ within the ZrP should be minimal, this would alter the π- π interactions of the $Ru(bpy)_3^{2+}$ within the layers thus affecting the overall quantum yield of the system. Moreover, due to the hydrophobic character of the quencher and the surface modifier, intercalation of p-BQ between the aliphatic chains is probable, resulting in an accumulation of p-BQ on the surface of the nanoparticles. The intercalation of the p-BQ is given by a driving force regime for the concentration of p-BQ in solution and the packing of the modifiers on the surface of the α-ZrP nanoparticles. The accumulation of the p-BQ on the surface creates a weak electronic interaction, acting as a static quencher even though there is no physical contact between the donor and acceptor and a physical barrier exists between them.[39] In addition, dynamic quenching can take place under two scenarios in this case study; the first happens

by the interaction of the $Ru(bpy)_3^{2+}$ on the edges of the particle and the p-BQ in solution and the second takes place by movement and migration of p-BQ and $Ru(bpy)_3^{2+}$ in the interlayer region.[40] Future work will be directed towards reducing the variables by fixing the quencher on the external surfaces.

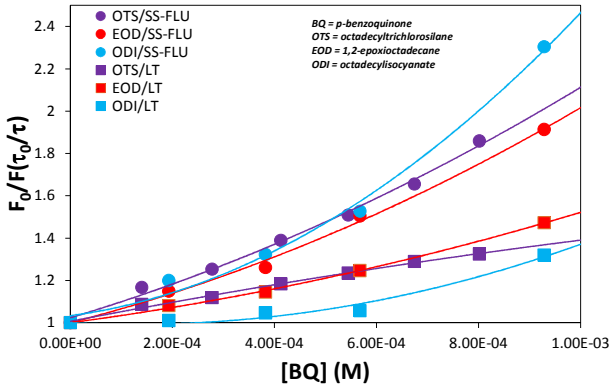

Figure 12: Stern-Volmer plot of the surface modified $Ru(bpy)_3^{2+}$@ZrP quenched by p-BQ in o-dichlorobenzene. [$Ru(bpy)_3^{2+}$@ZrP] = 0.01% m/v, λ_{em} = 595 nm, λ_{ex} = 450 nm.

Polymer nanocomposites

ZrP has found much use as a filler in polymeric materials over the years.[41, 42] The addition of the inorganic materials to the polymer matrix can largely impact the thermal and mechanical properties of the film. The typical goal in the preparation of such materials is to disperse individual nanosheets throughout the epoxy or polymer matrix; this has been predominantly been achieved two fashions. The initial approach is to exfoliate α-ZrP with long alkyl amines, in this case the individual nanosheets retain organic character as they interact with the amines and can therefore disperse within the organic matrix.[43] Another approach involves the use of amines to swell the layers of α-ZrP followed by treatment of the swollen α-

ZrP with a monomer.[42, 44] In this case the monomer is polymerized within the layers and the rapid growth of the polymer causes the exfoliation and dispersion of the particles within the matrix. The quality of the exfoliation and the orientation of the nanosheets greatly affect the properties of the resulting composite. In a special case, nafion, a cation exchanging polymer was exchanged with Zr(IV) and subsequently treated with phosphoric acid to produce α-ZrP nanocomposites in situ.[24, 45]

More recently organic modifications of α-ZrP have been used to synthesize fillers in polymers.[33, 46] In such cases organic groups can be incorporated directly into the α-ZrP by use of phosphate esters and phosphonic acids during the synthesis. In this case the length of the organic group dictates the strength of the interaction between the α-ZrP and the polymer. Additionally, the amount of phosphate and phosphonate can be varied to control the nature of the particle. Likewise organic modifications can be achieved after the synthesis of the α-ZrP material. Pica and co-workers have shown the organic modification of α-ZrP with aminoalcohols and phosphonic acids for the use as fillers in starch.[46, 47] In these cases the organic molecule interacts with the surface and the interlayer to produce an organically modified material.

Using the surface chemistry of α-ZrP it is now possible to prepare α-ZrP polymer composites in which the surface is compatible with the polymer and causes the particles to disperse within the matrix. The resulting materials are composed of unexfoliated α-ZrP dispersed in the polymer. Since the surface modification is exclusively on the surface of the nanoplatelets, the interlayer region is still free for further reaction and the interlayer can be used to add functionality to the

composite. Experiments were conducted in which α-ZrP surface modified with styrene oxide was intercalated with ammonium ion. It was found that loadings of up to 25% (w/w) could be achieved and that the transparency of the resulting films was maintained at loadings of up to 5% and the transparency was decreased at loadings above 10% (**Figure 13**).[31] Additionally, the dispersion of the intercalated nanoparticles within the polymer is confirmed by XRPD in which case diffraction is observed corresponding to the ammonium loaded phase of the nanoparticles. Additional experiments have shown that adjusting the loading of the ammonium ions results in a change of the transparency and thermal stability of the composites. In the case of lower ammonium loadings, the transparency is decreased relative to the fully loaded particles. The decrease in transparency is a direct result of the increase in the quantity of nanoparticles in the polymer matrix, resulting in agglomeration. This approach can be extended to a number of polymeric systems as the surface group can be tailored to interact with the polymer. Experiments with identical α-ZrP particles and loadings, but different functional groups showed the surface group does affect the thermal stability and dispersion of the nanofillers within the polymer. More information needs to be obtained about the mechanical strength of these composites as they are expected to behave much differently than materials produced with exfoliated α-ZrP.

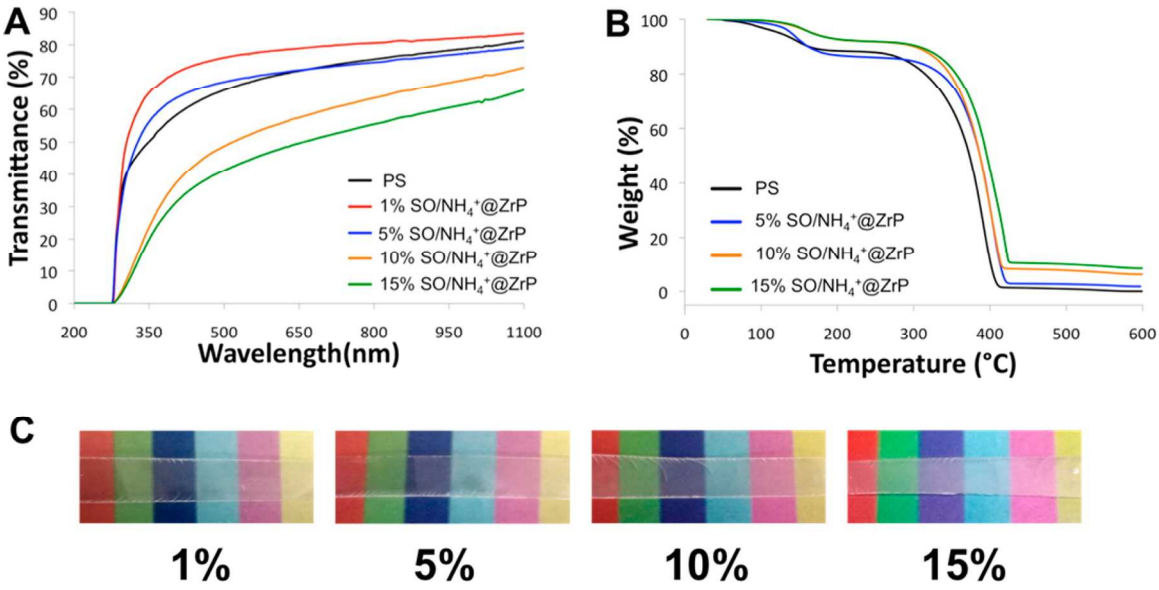

Figure 13: A) UV–visible spectra of the composite films showing the transparency of the composites at various nanofiller loadings. (B) TGA data of PS composite with SO/NH_4^+@ZrP displaying the delay in weight loss and increases thermal decomposition temperature, and (C) image of the composite films displaying the transparency of the composites. Taken from: Brian M. Mosby; Agustín Díaz; Vladimir Bakhmutov; Abraham Clearfield; *ACS Appl. Mater. Interfaces* **2014,** 6, 585-592.

Drug delivery

Recently, we have demonstrated the great potential of α-ZrP drug delivery applications. The intercalation of different drugs and proteins has been achieved with remarkable results.[48-50] The intercalated material is shielded from unwanted biological sites, until the nanoparticle reaches its desired target. This was the case for the intercalation of insulin into α-ZrP for example, in which an oral delivery of the peptidic hormone is desired.[48] The insulin was encapsulated into α-ZrP and protected from the low pH conditions of the stomach, but under neutral pH conditions of the intestine the insulin is quickly released, where it can be absorbed directly into the blood stream. Now, the surface modification of this system can

improve significantly the insulin release and further injection into the intestine. The use of a mucoadhesive coating should prolong the retention of the nanoparticles in the intestine for better insulin uptake, while penetrating species facilitates the insulin absorption. Furthermore, α-ZrP nanoparticles have been proven to be useful in the intercalation and delivery of a variety of anticancer chemotherapy agents in cancer nanotherapy.[49, 50] The biocompatibility of α-ZrP was evaluated in several cell lines (*i.e* human embryonic kidney cells (HEK-293), breast cancer cells (MCF-7), metastatic breast cancer cells (MDA-MB-231), among others) and the hemocompatibility of α-ZrP was evaluated with human red blood cells, showing no toxicity towards any of them.[50] Ultimately the α-ZrP nanoparticles themselves were shown to be biocompatible, hemocompatible and non-toxic to mouse macrophage cells (RAW 264.7).[48-50] The α-ZrP nanoplatelets were able to intercalate high loads of doxorubicin and cisplatin (up to 35% w/w or 33% molar ratio, and 20% w/w or 32% molar ratio, respectively) between their layers. Both are potent anticancer drugs used in chemotherapy. In addition, the loading of the drug in the nanoparticles can be tuned in order to obtain a specific release profile and/or dosification. The release of the drug was sustained for about 2 weeks in both cases and was dependent on pH. DOX@ZrP showed higher cellular uptake and increased cytotoxicity than free DOX in cancerous cells. Nevertheless, the surface modification of these chemotherapy nanoagents will have a profound impact on the targeting, distribution, degradation, and release of the nanoparticles. Specific polymer coatings can be used to improve solubility of the nanoparticles and retention time circulating in the body. Moreover, specific biomarkers can be included on the

surface of the nanoparticles to target a specific organ, tissue, or even type of cell. Mixed derivatives can be designed to control the release profile of the drug from the nanoparticles and the particle degradation rate. The multitude of possible surface modifications along with the many drugs that can be intercalated within the layers allows for the design of delivery vehicles to target specific sites within the body.

Colloidal stabilizers

The use of nanoparticles (such as clays, silica, asphaltenes or polymer based nanoparticles) as colloidal stabilizers by the so-called Pickering effect is well known and has been widely reported in the literature.[30, 51-55] The basic concept of the Pickering effect resides in the ability of the nanoparticles to become trapped at the interphase of the colloidal mixture, partially isolating the two phases consequently decreasing the interfacial tension between the two different phases making a stable mixture. Nevertheless, this process is basically governed by three factors; particle size, shape, and polarity. The use of two-dimensional nanoparticles with high aspect ratios, or nanosheets, has been demonstrated to be a successful model for Pickering emulsions, due to the fact that capillary pressures at the interphase kept them sequestered at the interphase, making a very stable colloidal solution.[30, 54]

In order to improve the interaction of the nanoparticles with each of the two phases, surface modifiers with amphiphilic characters can be employed, modifying their polarity character. In addition, several α-ZrP nanoparticles with different aspect ratios can be employed to exploit their Pickering's properties.[35] Cheng and coworkers reported the use of exfoliated α-ZrP by propylamine to stabilize an air-in-

water foam with remarkable results.[54] These authors reported that the surface coverage and aspect ratio of the α-ZrP nanosheets affects the stability of the aqueous foam, where the nanosheets prevent the diffusion of air between bubbles, inhibiting Ostwald ripening and coalescence. On the other hand, surface modification controlled synthesis followed by an exfoliation reaction produces Janus and Gemini nanosheets.[30] In our own efforts, we produced Janus and Gemini nanosheets that act as a nanosurfactant with an anisotropical amphiphilic character at the interphase of an oil-in-water emulsion, showing a remarkable stability.[30]

6. Conclusion

It has been demonstrated that α-ZrP can be successfully surface modified with a number of different reactive molecules. The coordination of the ligand to the surface dictates the uptake of the organic modifier and therefore the reactive group can be changed in order to control the uptake of ligand. Additionally, it was shown that surface modification is possible with α-ZrP of various sizes, however as the thickness of the particles increases the percentage of modified phosphorus in the compound decreases. Lastly, the full characterization of multifunctional α-ZrP based materials prepared by coupling intercalation and surface modification was presented. Although the field of surface chemistry has been largely growing, layered materials have not gained much exposure. The interlayer of these materials gives them properties that differ greatly from typical materials and allows the opportunity for further functionalization. Although α-ZrP was presented in this article, similar chemistry can be achieved for other layered materials. The synthesis

of multifunctional nanoparticles from layered materials should therefore be a large field of interest leading to many unique applications.

Acknowledgments:

This work was supported by the Texas A&M University Graduate Diversity Fellowship (B.M.M.), the Robert A. Welch Foundation Grant No. A-0673, the National Science Foundation Grant # DMR-0652166, and the US Department of Energy Grant DE-FG02-03ER15420, for which grateful is made. We also acknowledge the X-ray Diffraction Laboratory at Texas A&M University for the use of the X-ray powder diffractometer. We acknowledge Dr. Angel Martí for his help with the steady-state fluorescent and transient lifetime measurements at the Department of Chemistry at Rice University, and for his help in the data interpretation. We also acknowledge Dr. Vladimir Bakhmoutov at the Chemistry NMR Laboratory for assistance with the solid-state NMR experiments.

References

1. J. H. de Boer, *Z. Anorg. Allg. Chem.*, 1925, 144, 190-196.
2. K. A. Kraus and H. O. Phillips, *J. Am. Chem. Soc.*, 1956, 78, 694-694.
3. K. A. Kraus, H. D. Phillips, T. A. Carlson and J. S. Johnson, 1958.
4. C. B. Amphlett, L. A. Mcdonald and M. J. Redman, *J. Inorg. Nucl. Chem.*, 1958, 6, 220-235.
5. W. B. Blumenthal, *Ind. Eng. Chem.*, 1954, 46, 528-539.
6. A. Clearfield and J. A. Stynes, *J. Inorg. Nucl. Chem.*, 1964, 26, 117-129.
7. A. Clearfield and G. D. Smith, *Inorg. Chem.*, 1969, 8, 431-436.
8. J. M. Troup and A. Clearfield, *Inorg. Chem.*, 1977, 16, 3311-3314.
9. A. Clearfield, R. H. Blessing and J. A. Stynes, *J. Inorg. Nucl. Chem.*, 1968, 30, 2249-2258.
10. A. N. Christensen, E. K. Andersen, I. G. K. Andersen, G. Alberti, M. Nielsen and M. S. Lehmann, *Acta. Chem. Scand.*, 1990, 44, 865-872.

11. D. M. Poojary, B. Shpeizer and A. Clearfield, *J. Chem. Soc., Dalton Trans.*, 1995, 111-113.
12. A. Clearfield and U. Costantino, in *Comprehensive Supramolecular Chemistry* eds. G. Alberti and T. Bein, Pergamon Press, 1996, vol. 7, pp. 107-149.
13. A. Clearfield and K. Demadis, eds., *Metal Phosphonate Chemistry: From Synthesis to Applications*, RSC Publishing:, Cambridge, UK, 2012.
14. A. Diaz, B. M. Mosby, V. I. Bakhmutov, A. A. Marti, J. D. Batteas and A. Clearfield, *Chem. Mater.*, 2013, 25, 723-728.
15. A. Clearfield, A. Oskarsson and C. Oskarsson, *Ion Exch. Membr.*, 1972, 1, 91-107.
16. L. Y. Sun, W. J. Boo, H. J. Sue and A. Clearfield, *New J. Chem.*, 2007, 31, 39-43.
17. G. Alberti, U. Costantino and R. Giulietti, *J. Inorg. Nucl. Chem.*, 1980, 42, 1062-1063.
18. M. Pica, A. Donnadio, D. Capitani, R. Vivani, E. Troni and M. Casciola, *Inorg. Chem.*, 2011, 50, 11623-11630.
19. G. Alberti, U. Costantino, S. Allulli and N. Tomassini, *J. Inorg. Nucl. Chem.*, 1978, 40, 1113-1117.
20. A. Clearfield, *Nanoparticles: Group IV Phosphonates*, Imperial College Press, London, UK, 2nd edn., 2012.
21. M. D. Poojary, H. L. Hu, F. L. Campbell, III and A. Clearfield, *Acta Crystallogr., Sect. B: Struct. Sci.*, 1993, B49, 996-1001.
22. A. Clearfield, *Inorg. Chem.*, 1964, 3, 146-148.
23. A. Clearfield, *Dalton Trans.*, 2008, 6089-6102.
24. M. Casciola, G. Bagnasco, A. Donnadio, L. Micoli, M. Pica, M. Sganappa and M. Turco, *Fuel Cells*, 2009, 9, 394-400.
25. M. B. Santiago, C. Declet-Flores, A. Díaz, M. M. Vélez, M. Z. Bosques, Y. Sanakis and J. L. Colón, *Langmuir*, 2007, 23, 7810-7817.
26. E. Brunet, M. Alonso, C. Cerro, O. Juanes, J. C. Rodriguez-Ubis and A. E. Kaifer, *Adv. Funct. Mater.*, 2007, 17, 1603-1610.
27. A. Pattammattel, I. K. Deshapriya, R. Chowdhury and C. V. Kumar, *Langmuir*, 2013, 29, 2971-2981.
28. X. He, H. Xiao, H. Choi, A. Díaz, B. Mosby, A. Clearfield and H. Liang, *Colloids Surf., A*, 2014, DOI: 10.1016/j.colsurfa.2014.1003.1041.
29. V. F. D. Alvaro and R. A. W. Johnstone, *J. Mol. Catal. A:Chem.*, 2008, 280, 131-141.
30. A. F. Mejia, A. Diaz, S. Pullela, Y.-W. Chang, M. Simonetty, C. Carpenter, J. D. Batteas, M. S. Mannan, A. Clearfield and Z. Cheng, *Soft Matter*, 2012, 8, 10245-10253.
31. B. M. Mosby, A. Díaz, V. Bakhmutov and A. Clearfield, *ACS Appl. Mater. Inter.*, 2014, 6, 585-592.
32. B. M. Mosby, M. Goloby, A. Diaz, V. I. Bakhmutov and A. Clearfield, *Langmuir*, 2014, 30, 2513-2521.
33. M. Casciola, D. Capitani, A. Donnadio, G. Munari and M. Pica, *Inorg. Chem.*, 2010, 49, 3329-3336.
34. Q. Liu, J. R. de Wijn, K. de Groot and C. A. van Blitterswijk, *Biomaterials*, 1998, 19, 1067-1072.

35. L. Sun, W. J. Boo, H.-J. Sue and A. Clearfield, *New J. Chem.*, 2007, 31, 39-43.
36. J. D. Wang, A. Clearfield and G.-Z. Peng, *Mater. Chem. Phys.*, 1993, 35, 208-216.
37. C. Y. Ortiz-Avila and A. Clearfield, *Inorg. Chem.*, 1985, 24, 1773-1778.
38. A. Clearfield and C. Y. Ortiz-Avila, in *Supramolecular Architecture*, American Chemical Society, 1992, vol. 499, ch. 14, pp. 178-193.
39. M. Porel, S. Jockusch, A. Parthasarathy, V. J. Rao, N. J. Turro and V. Ramamurthy, *Chem. Commun. (Cambridge, U. K.)*, 2012, 48, 2710-2712.
40. A. A. Mart and J. L. Colón, *Inorg. Chem.*, 2010, 49, 7298-7303.
41. L. Y. Sun, J. Liu, S. R. Kirumakki, E. D. Schwerdtfeger, R. J. Howell, K. Al-Bahily, S. A. Miller, A. Clearfield and H. J. Sue, *Chem. Mater.*, 2009, 21, 1154-1161.
42. H. J. Sue, K. T. Gam, N. Bestaoui, N. Spurr and A. Clearfield, *Chem. Mater.*, 2004, 16, 242-249.
43. L. Sun, W. J. Boo, D. Sun, A. Clearfield and H.-J. Sue, *Chem. Mater.*, 2007, 19, 1749-1754.
44. W. J. Boo, L. Sun, J. Liu, A. Clearfield and H.-J. Sue, *J. Phys. Chem. C*, 2007, 111, 10377-10381.
45. M. Casciola, D. Capitani, A. Comite, A. Donnadio, V. Frittella, M. Pica, M. Sganappa and A. Varzi, *Fuel Cells*, 2008, 8, 217-224.
46. M. Pica, A. Donnadio, E. Troni, D. Capitani and M. Casciola, *Inorg. Chem.*, 2013, 52, 7680-7687.
47. M. Pica, A. Donnadio and M. Casciola, *Starch - Stärke*, 2012, 64, 237-245.
48. A. Díaz, A. David, R. Pérez, M. L. González, A. Báez, S. E. Wark, P. Zhang, A. Clearfield and J. L. Colón, *Biomacromolecules*, 2010, 11, 2465-2470.
49. A. Díaz, V. Saxena, J. Gonzalez, A. David, B. Casanas, C. Carpenter, J. D. Batteas, J. L. Colón, A. Clearfield and M. Delwar Hussain, *Chem. Commun.*, 2012, 48, 1754-1756.
50. V. Saxena, A. Diaz, A. Clearfield, J. D. Batteas and M. D. Hussain, *Nanoscale*, 2013, 5, 2328-2336.
51. S. U. Pickering, *J. Chem. Soc., Dalton Trans.*, 1907, 91, 2001-2021.
52. M. Reger, T. Sekine, T. Okamoto, K. Watanabe and H. Hoffmann, *Soft Matter*, 2011, 7, 11021-11030.
53. M. Reger, T. Sekine and H. Hoffmann, *Colloids Surf., A*, 2012, 413, 25-32.
54. J. S. Guevara, A. F. Mejia, M. Shuai, Y.-W. Chang, M. S. Mannan and Z. Cheng, *Soft Matter*, 2013, 9, 1327-1336.
55. K. Y. Tan, J. E. Gautrot and W. T. S. Huck, *Langmuir*, 2010, 27, 1251-1259.

Surface Modification of Layered Zirconium Phosphates: A Novel Pathway to Multifunctional Materials

*Brian M. Mosby, Agustín Díaz, and Abraham Clearfield**

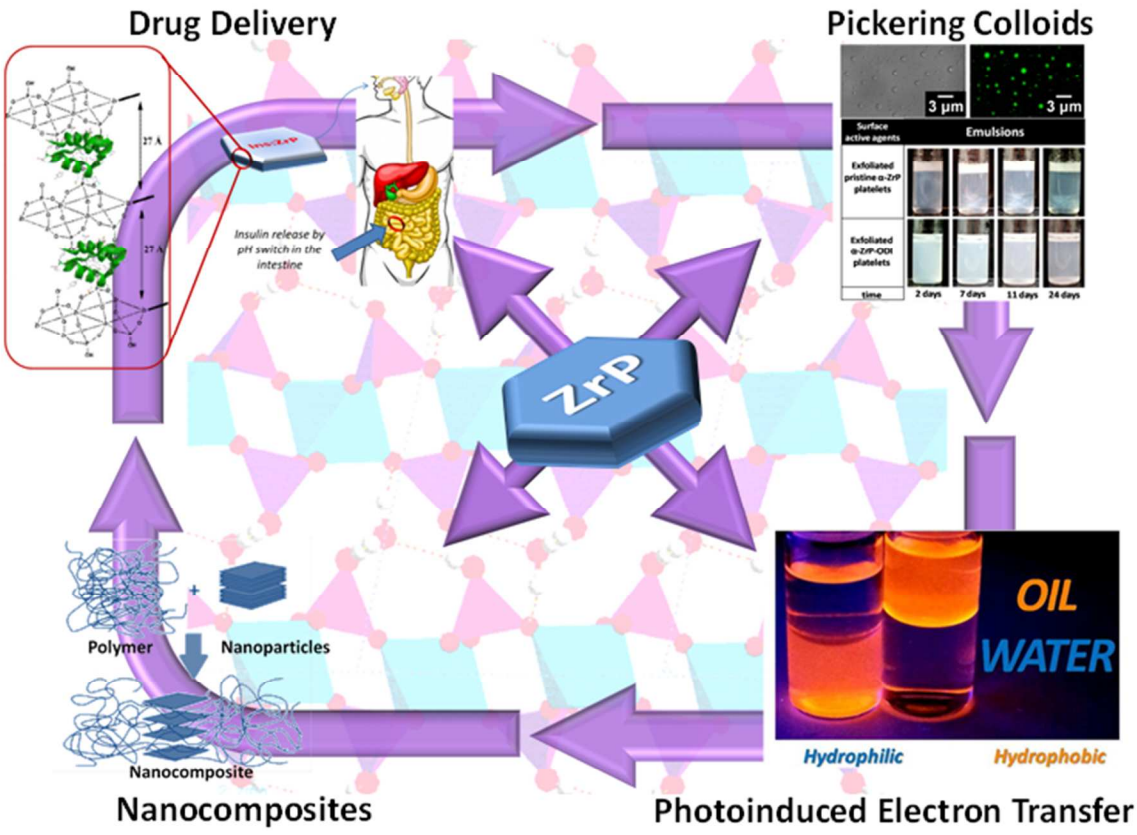

Combination of surface modification and intercalation chemistry of inorganic layered materials allows for the design of nanoparticles for specific applications.